



Supported by



Accepted Article

Title: Porous Boron Nitride as a Weak Solid Base Catalyst

Authors: Shohei Nakamura, Atsushi Takagaki, Motonori Watanabe,
Kanta Yamada, Masaaki Yoshida, and Tatsumi Ishihara

This manuscript has been accepted after peer review and appears as an Accepted Article online prior to editing, proofing, and formal publication of the final Version of Record (VoR). This work is currently citable by using the Digital Object Identifier (DOI) given below. The VoR will be published online in Early View as soon as possible and may be different to this Accepted Article as a result of editing. Readers should obtain the VoR from the journal website shown below when it is published to ensure accuracy of information. The authors are responsible for the content of this Accepted Article.

To be cited as: *ChemCatChem* 10.1002/cctc.202001435

Link to VoR: <https://doi.org/10.1002/cctc.202001435>

Porous Boron Nitride as a Weak Solid Base Catalyst

Shohei Nakamura,^[b] Atsushi Takagaki*^[a,c], Motonori Watanabe,^[a,b,c] Kanta Yamada,^[d] Masaaki Yoshida,^[d,e] and Tatsumi Ishihara*^[a]

- [a] Prof. A. Takagaki, Prof. M. Watanabe, Prof. T. Ishihara
Department of Applied Chemistry, Faculty of Engineering
Kyushu University
744 Motoooka, Nishi-ku, Fukuoka 819-0395, Japan
E-mail: atakagak@cstf.kyushu-u.ac.jp, ishihara@cstf.kyushu-u.ac.jp
- [b] S. Nakamura, Prof. M. Watanabe, Prof. T. Ishihara
Department of Automotive Science, Graduate School of Integrated Frontier Sciences
Kyushu University
744 Motoooka, Nishi-ku, Fukuoka 819-0395, Japan
- [c] Prof. A. Takagaki, Prof. M. Watanabe, Prof. T. Ishihara
International Institute for Carbon-Neutral Energy Research (WPI-I²CNER)
Kyushu University
744 Motoooka, Nishi-ku, Fukuoka 819-0395, Japan
- [d] K. Yamada, Prof. M. Yoshida
Graduate School of Sciences and Technology for Innovation,
Yamaguchi University
Tokiwadai, Ube, Yamaguchi 755-8611, Japan
- [e] Prof. M. Yoshida
Blue Energy Center for SGE Technology (BEST)
Yamaguchi University
Tokiwadai, Ube, Yamaguchi 755-8611, Japan

Abstract: Porous boron nitride was synthesized by pyrolysis from boric acid and urea mixed in varying molar ratios. The boron nitride prepared had high surface areas ranging from 376 to 647 m² g⁻¹ with both microporous and mesoporous structures. The sample prepared with a urea-to-boric acid molar ratio of 5 exhibited the highest pore volume with the highest surface area of mesopores. Boron-K edge X-ray absorption fine structure spectroscopy revealed that the surface structure consisted of BN₃ sites along with BN₂O, BNO₂, and BO₃ sites. Fourier transform infrared (FTIR) spectroscopy indicated the formation of amino and hydroxyl groups on the surface. Analysis using color indicator reagents and deuterated chloroform-adsorbed FTIR results indicated that the porous boron nitride had very weak base sites of strength +7.2 > H_a ≥ +6.3. Porous boron nitride exhibited a high activity for the nitroaldol reaction with a high selectivity for nitroalkene (>97%). A good correlation was observed between the catalytic activity of the boron nitride catalysts and their porous structures.

Introduction

Acid and base catalysts are essential for the production of fuels and chemicals in both the established petrochemical industry and emerging biorefineries. Solid acid and base catalysts are easily separated from the reaction solution and can be used for further reactions without neutralization so that the replacement of liquid acids and bases with their solid counterparts offers environmental and economic benefits. While many types of solid acids such as zeolites, metal oxides, and sulfonated ion-exchange resins have been developed, and some of them are commercially available,^[1] the use of solid bases such as alkaline earth metal oxides has been limited. This is mainly owing to the poisoning of the catalyst with water and CO₂ and the difficulty in controlling base-catalyzed reactions in which side reactions typically occur in series and parallel, resulting in insufficient selectivity to the desired products.^[2] Thus, the development of solid base catalysts is still required.

While boron nitride has so far been mainly regarded as an inert material, it has recently attracted much attention as a novel heterogeneous catalyst.^[3-8] Hexagonal boron nitride and its nanotubes and nanosheets were found to catalyze oxidative dehydrogenation of light alkanes to the corresponding alkenes with excellent selectivity, much superior to that of other catalysts such as supported vanadium oxide and carbon nanotubes.^[3] Also, boron nitride could activate methane to give CO and C₂ products with minor formation of CO₂.^[4] Moreover, boron nitride was found to function as a photocatalyst for hydrogen production^[5] and CO₂ reduction.^[6] Currently, boron nitride is recognized to have a variety of interesting catalytic functionalities in addition to exhibiting excellent properties as catalyst support.^[9,10]

Here, we synthesized porous boron nitride for use as solid base catalysts. Porous boron nitride was synthesized by condensation of boric acid (H₃BO₃) and urea (CO(NH₂)₂), followed by pyrolysis. The prepared materials had high surface areas with both micro- and mesopores. The boron nitride catalyst exhibited catalytic activity for the nitroaldol reaction and selectively yielded nitroalkene, which possesses a high synthetic potential in organic chemistry, whereas conventional strong bases such as CaO and Mg-Al hydrotalcite did not. The physicochemical and solid base properties of the synthesized boron nitride were characterized through a variety of techniques. The correlation between the catalytic activities of the boron nitride catalysts and their other properties was investigated.

Results and Discussion

Porous boron nitride was synthesized as follows. 10 mmol of boric acid and 50 mmol of urea were dissolved in 100 mL of water. The solution was then evaporated to dryness. The precursor powder obtained (ca. 3 g) was transferred to an alumina boat and heated at 1273 K for 3 h in an NH₃ flow (100 cm³ (NTP) min⁻¹). The final product was a white powder.

Synthesis was also carried out by using varying molar ratios of boric acid to urea, namely, 1:2, 1:5, 1:10, and 1:15. The synthesized boron nitride is denoted as BN(1:n).

Figure 1 shows the X-ray diffraction (XRD) patterns for boron nitride samples synthesized from boric acid and urea mixed at different molar ratios. All samples exhibited two diffraction peaks corresponding to the (002) and (100) reflections of turbostratic boron nitride (*t*-BN), which was in good agreement with previous reports.^[11] An increase in the molar ratio of urea broadened the (002) diffraction peak, indicating lower crystallinity. Table 1 shows the crystallite sizes calculated from the (002) and (100) reflections using the Scherrer equation. The crystallite sizes for BN(1:2) were 1.1 and 2.8 nm from the (002) and (100) diffractions, respectively. The difference between the two crystallite sizes is due to the anisotropy of the layered materials. With increasing urea content, the crystallite size, as determined from the (002) diffraction, decreased monotonically from 1.1 to 0.7 nm. The average numbers of layers were roughly estimated to be 3 for BN(1:2) and 2 for BN(1:15). The decrease in the thickness of layers was in good agreement with the results of a previous study.^[12]

Table 1 lists the elemental compositions of the boron nitride samples determined by energy-dispersive X-ray spectroscopy (EDX). As desired, the synthesized samples consisted of boron and nitrogen with a small amount of carbon and oxygen. The elemental compositions of the synthesized samples were roughly the same except for BN(1:2).

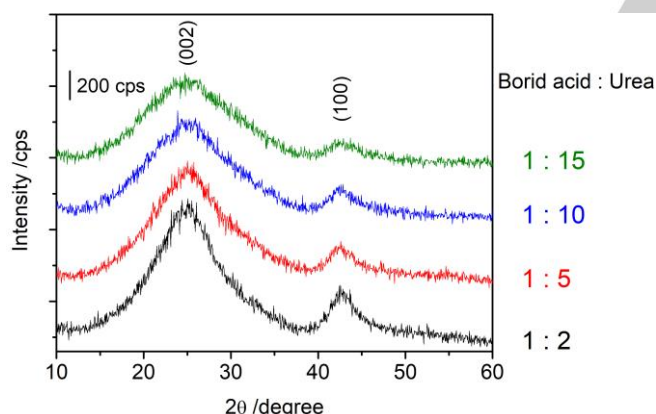


Figure 1. XRD patterns for boron nitride samples synthesized from boric acid and urea at various molar ratios.

Table 1. Crystallite sizes and elemental compositions of the synthesized boron nitride.

| Sample | Crystallite size /nm ^[a] | | Atomic conc./% ^[b] | | | |
|----------|-------------------------------------|-------|-------------------------------|----|----|----|
| | (002) | (100) | B | C | N | O |
| BN(1:2) | 1.1 | 2.8 | 36 | 14 | 40 | 10 |
| BN(1:5) | 0.9 | 3.1 | 45 | 13 | 38 | 5 |
| BN(1:10) | 0.8 | 3.0 | 44 | 13 | 35 | 8 |
| BN(1:15) | 0.7 | 2.6 | 45 | 13 | 39 | 4 |

[a] Calculated by Scherrer equation. [b] From EDX.

Figure 2 shows scanning electron microscopy (SEM) images of boron nitride samples. Aggregates of very small particles were observed for BN(1:2) (Fig. 2(a)). With increasing urea content, the surface morphology changed drastically, leading to the formation of mesopores. Pores less than 20 nm in size were observed in BN(1:5) (Fig. 2(b)). Similar morphologies were obtained in the case of BN(1:10) and BN(1:15) (Figs. 2(c,d)). It seems that the pores in BN(1:10) were larger than those in BN(1:5). These pores could have been formed as a result of the evaporation of the excess urea that could not be condensed with boric acid during synthesis.

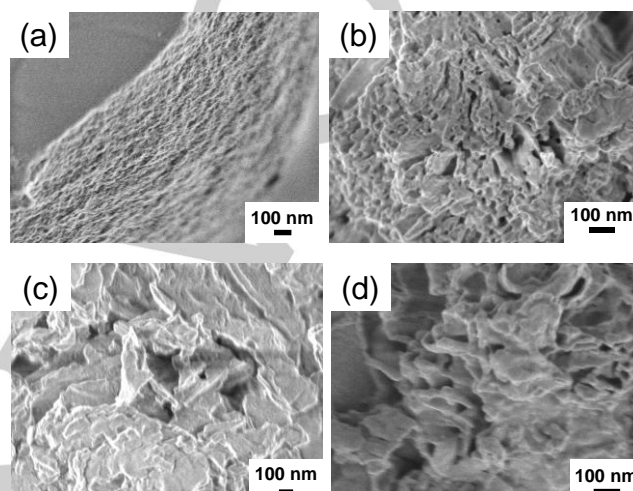


Figure 2. SEM images of boron nitride synthesized from boric acid and urea at various molar ratios. (a) BN(1:2), (b) BN(1:5), (c) BN(1:10), and (d) BN(1:15).

The porous structure of the synthesized samples was investigated by nitrogen adsorption measurements. Figure 3 shows nitrogen sorption isotherms and pore size distributions obtained from Barrett-Joyner-Halenda (BJH) plots. Table 2 shows the BET surface areas and pore volumes of the synthesized samples. The surface areas of the synthesized BN samples were significantly higher than that of commercial BN (6 m² g⁻¹). The BET surface area of BN(1:2) was 376 m² g⁻¹, and the surface areas of BN(1:5) and BN(1:10) were even higher: 496 and 647 m² g⁻¹, respectively. The BET surface area decreased to 483 m² g⁻¹ for BN(1:15). The nitrogen sorption isotherms indicated that the synthesized BN had micropores. The micropore structure was characterized further by using the *t*-plot method. The surface area of micropores (*S*_{micro}) was 370 m² g⁻¹ for BN(1:2), which was close to the BET surface area, 376 m² g⁻¹, indicating that most of the pores of BN(1:2) were inside the particles as corroborated by the SEM image (Fig. 2). BN(1:5) had both micro- and mesopores, resulting in the highest pore volume (1.24 mL g⁻¹) and highest external surface area (*S*_{ext}, 160 m² g⁻¹) among the samples prepared. The pore size distribution for BN(1:5) clearly showed evidence of mesopores centered at 12 nm, which is in good agreement with the SEM image. The BN(1:10) sample had the highest surface area of micropores, which led to the highest total surface area but a lower pore volume than BN(1:5).

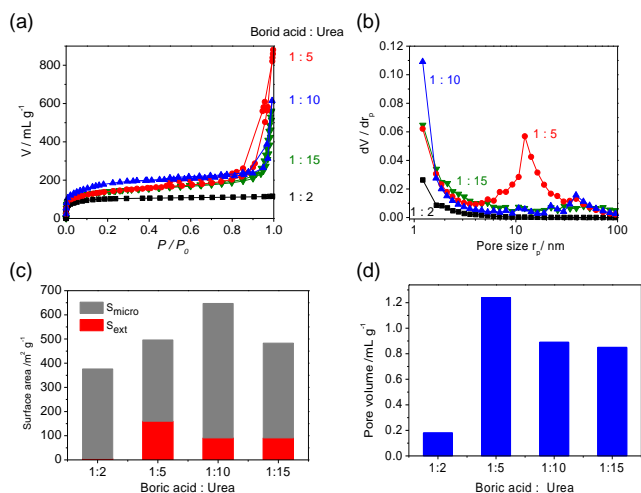


Figure 3. (a) N_2 sorption isotherms, (b) pore size distributions, (c) surface areas, and (d) pore volumes of the synthesized boron nitride.

Table 2. Surface areas, pore sizes, and pore volumes of the synthesized boron nitride.

| Sample | S_{BET} /m ² g ⁻¹ | S_{micro} /m ² g ⁻¹ | S_{ext} /m ² g ⁻¹ | Pore volume /mL g ⁻¹ |
|----------|---|---|---|------------------------------------|
| BN(1:2) | 376 | 370 | 6 | 0.18 |
| BN(1:5) | 496 | 336 | 160 | 1.24 |
| BN(1:10) | 647 | 556 | 91 | 0.89 |
| BN(1:15) | 483 | 392 | 91 | 0.85 |

Figure 4 shows the FTIR spectra of the synthesized samples. The characteristic absorption for boron nitride was occurred at 1372 and 816 cm^{-1} . The former strong absorption corresponds to B-N stretching, and the latter to B-N-B bending.^[12-14] All samples produced these bands, indicating the formation of boron nitride, as confirmed by XRD. In addition, a broad band around 3400 cm^{-1} with a shoulder around 3200 cm^{-1} was observed. These are attributed to O-H stretching vibrations and N-H stretching vibrations, respectively, indicating the formation of amino and hydroxyl groups.^[12, 15-17]

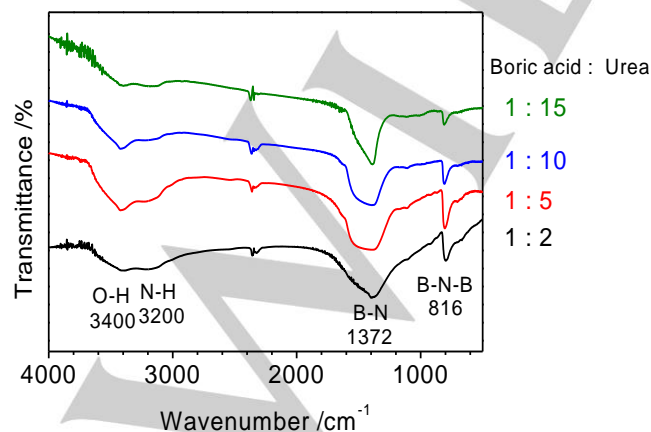


Figure 4. FTIR spectra for synthesized boron nitride.

Figure 5 shows the B-K edge XAFS spectra for the synthesized boron nitride. The spectra for commercial boron nitride and boron oxide (B_2O_3) are shown for reference. The B-K edge XAFS spectra were measured by the surface-sensitive total electron yield method. The spectrum of commercial hexagonal boron nitride had a single peak at 192.0 eV, which is attributable to the excitation of B1s electrons to $\pi^*(BN_3)$, whereas the spectrum of boron oxide showed a peak at 194.0 eV, ascribed to excitation to $\pi^*(BO_3)$.^[18-21] For BN(1:5), BN(1:10), and BN(1:15), in addition to the strong excitation of B1s electrons to $\pi^*(BN_3)$, weak excitations to $\pi^*(BN_2O)$, $\pi^*(BNO_2)$, and $\pi^*(BO_3)$ were observed.^[22,23] This indicated that the surface of these materials had BN_3 sites along with BN_2O , BNO_2 , and BO_3 sites, which was related to the formation of amino and hydroxyl groups on the surface, as revealed by FTIR spectroscopy. Note that the spectra were not influenced by the presence of hydrogen. For example, the BN_2O sites could comprise N-B(N)-OH and NH_2 -B(N)-OH. In contrast, for BN(1:2), a strong peak for BO_3 sites was observed, indicating that the surface of BN(1:2) was mostly hydroxylated, even though XRD indicated a boron nitride structure. The difference of oxygen contents observed between EDX and B-K edge XAFS is due to the surface sensitivity of the XAFS spectra. The detection method used in this measurement probes to a depth of about 0.6 nm from the surface.^[24,25]

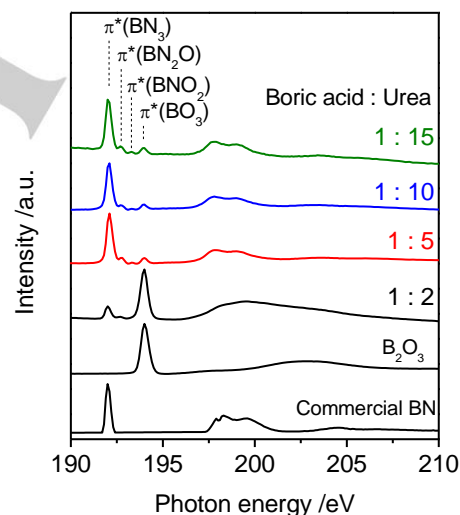


Figure 5. B K-edge XAFS spectra for synthesized boron nitride.

Solid base properties of the synthesized boron nitride samples were examined using color indicator reagents and $CDCl_3$ -adsorbed FTIR measurements. Two color indicator reagents, bromocresol purple ($pK_a = +6.3$) and bromothymol blue ($pK_a = +7.2$), were used. The coloration by bromocresol purple was observed for all samples, revealing that the synthesized boron nitride samples had weak base sites with $H_- \geq +6.3$. When treated with a solution containing bromothymol blue, BN(1:5) turned green, whereas the other samples turned yellow, indicating that BN(1:5) had base sites of strength $H_- \geq +7.2$ while the other BN samples had very weak base sites of strength $+7.2 > H_- \geq +6.3$. The amounts of base sites, estimated by titration with benzoic acid, were 0.10, 0.22, 0.21, and 0.12

mmol g⁻¹ for BN(1:2), BN (1:5), BN (1:10), and BN (1:15), respectively.

The base strength was also determined by using CDCl₃-adsorbed FTIR measurements. Figure 6 shows the difference FTIR spectrum for CDCl₃-adsorbed boron nitride. The C-D stretching band was observed at 2252 cm⁻¹. It has been reported that the observed frequency of the C-D band for CDCl₃ adsorbed on silica was 2265 cm⁻¹;^[26] the corresponding values were 2253 cm⁻¹ on γ-Al₂O₃,^[27] and 2245 and 2220 cm⁻¹ on MgO.^[28] Thus, BN had weak base sites, stronger than SiO₂, comparable to Al₂O₃, but much weaker than MgO.

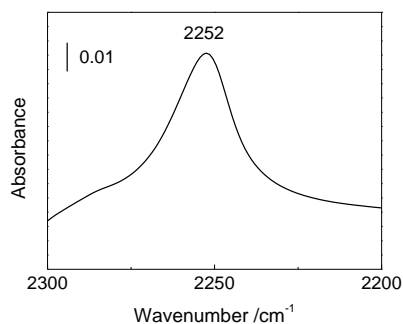
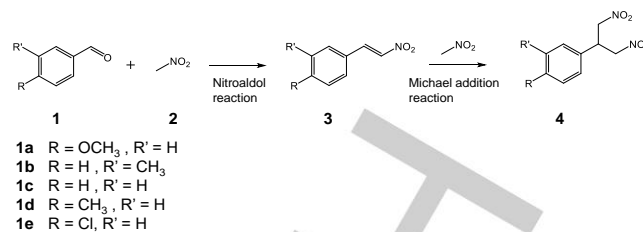


Figure 6. Difference FTIR spectrum of CDCl₃-adsorbed boron nitride.

The base catalytic activity of boron nitride was determined through the nitroaldol reaction (Scheme 1). Table 3 lists the results of the nitroaldol reaction for the synthesized boron nitride. The synthesized BN showed high activities (entries 1-4), while commercial BN (h-BN) was inactive for the reaction (entry 5). Notably, BN(1:5) gave the highest conversion of *p*-methoxybenzaldehyde (**1a**) with excellent selectivity to the corresponding nitroalkene (**3a**) (97%) (entry 2). The BN(1:5) sample was also synthesized in Ar atmosphere instead of NH₃, and used for the reaction. The sample also exhibited a high **1a** conversion of 93% with a selectivity to **3a** (71%). BN(1:10) and BN(1:15) also exhibited similarly high selectivities to the nitroalkene (97 and 99%) (entries 3 and 4). In contrast, BN(1:2) showed a lower conversion and selectivity than other boron nitride catalysts. These results suggest that the surface amino groups functioned as base sites for the reaction. Conventional solid bases such as CaO, Mg-Al hydrotalcite, and γ-Al₂O₃ were used for comparison. The strong solid bases CaO and hydrotalcite yielded a dinitro compound **4a**, rather than nitroalkene **3a** because of the subsequent Michael addition reaction (entries 6 and 7). The difference between conversion and sum of two products is probably due to adsorption of the reactant on the catalyst and degradation of the reactant. A weaker solid base, γ-Al₂O₃, could yield nitroalkene **3a**, but the conversion and selectivity were much lower than those for boron nitride. It can be concluded that weak base sites of boron nitride were effective for selective formation of nitroalkene. It is reported that strong basic sites are not necessary for the nitroaldol reaction because the abstraction of a proton from nitromethane is easy.^[29]



Scheme 1. Nitroaldol reaction of substituted benzaldehyde and nitromethane, and the subsequent Michael addition reaction.

Table 3. Results of nitroaldol reaction of nitromethane and *p*-methoxybenzaldehyde using synthesized boron nitride.^[a]

| Entry | Catalyst | 1a Conv. /% | Selectivity /% | |
|-------|---|----------------|----------------|----|
| | | | 3a | 4a |
| 1 | BN(1:2) | 16 | 52 | 0 |
| 2 | BN(1:5) | 83 | 97 | 0 |
| 3 | BN(1:10) | 77 | 97 | 1 |
| 4 | BN(1:15) | 58 | 99 | 0 |
| 5 | h-BN ^[b] | 26 | 3 | 3 |
| 6 | CaO ^[c] | 22 | 4 | 12 |
| 7 | Mg-Al hydrotalcite ^[d] | 28 | 20 | 63 |
| 8 | γ-Al ₂ O ₃ ^[e] | 43 | 77 | 4 |

[a] Reaction conditions: **1a** (0.5 mmol), **2a** (1.25 mmol), catalyst (50 mg), *n*-decane (0.1 mmol), toluene (2 mL), 393 K, 30 h. [b] Commercial boron nitride (Wako), S_{BET}; 6 m² g⁻¹. [c] Pretreated at 973 K for 3 h. S_{BET}; 8 m² g⁻¹. [d] Mg/Al = 3. Pretreated at 773 K for 3 h. S_{BET}; 219 m² g⁻¹. [e] S_{BET}; 88 m² g⁻¹.

Figure 7 shows time-course of the reaction over BN(1:5) and the results of its recycle use. The reaction smoothly proceeded, indicating that both adsorption of the reactant and desorption of the products satisfactorily occurred. For the recyclability test, the catalysts were collected by centrifugation at 3000 rpm, washed with 10 mL of toluene three times, dried overnight, and reused for further reactions. It was found that the activity gradually decreased. The **3a** yield after 3rd reuse was 58%.

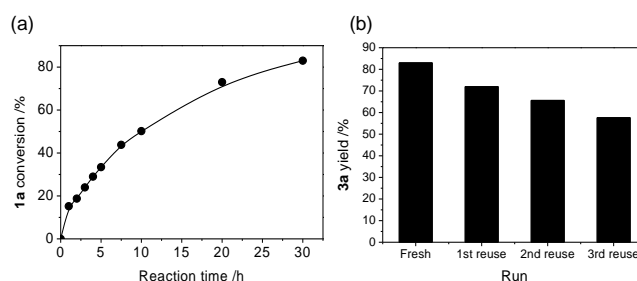


Figure 7. (a) Time course of nitroaldol reaction over BN(1:5) and (b) recycle use of BN(1:5) Reaction conditions: **1a** (0.5 mmol), **2a** (1.25 mmol), BN(1:5) (50 mg), *n*-decane (0.1 mmol), toluene (2 mL), 393 K, 30 h.

The scope of the reaction was investigated by using various substituted benzaldehydes. Table 4 lists the results of reaction rate of the nitroaldol reaction. It was found that the substrates with electron-withdrawing groups such as *m*-methoxy benzaldehyde (**1b**) and *p*-chloro benzaldehyde (**1e**) exhibited higher activity than benzaldehyde (**1c**). This trend is the same as that over alkaline-cation exchanged zeolite.^[30] Surprisingly, it was found that the substrates with electron-donating groups including *p*-methoxy benzaldehyde (**1a**) and *p*-tolualdehyde (**1d**) also showed higher reaction rate than benzaldehyde (**1c**). Figure 8 shows the Hammett plot for the nitroaldol reaction over BN(1:5) catalyst. As the results, the V-shaped plot was observed over the porous boron nitride catalysts while the plot with a positive value of slope was obtained over basic zeolites.^[30] The concave upward curve indicates a change in the reaction mechanism.^[31] Scheme 2 shows proposed two different reaction mechanisms, base mechanism, and acid-base cooperative mechanism. The base catalyzed mechanism is a general one which involves a proton abstraction of nitromethane by base sites, amino groups on the boron nitride in this case, a nucleophilic attack of the deprotonated nitromethane to benzaldehyde, and subsequent dehydration to form nitroalkene. The substrates with electron-withdrawing groups which have positive values of the Hammett constants would follow this mechanism because they are susceptible to the nucleophilic attack, resulting in the positive value of slope in the Hammett plot.

As for the substrates with electron-donating groups which showed the negative value of slope in the Hammett plot, the acid-base cooperative mechanism is proposed. We have previously investigated a solid base activity of a ball-milled boron nitride and obtained a negative value of slope for the Hammett plot.^[32] It is considered that electron-donating groups stimulated the polarization of the carbonyl group of benzaldehyde by the resonance effect (Scheme 2(c)) and enhanced the interaction with the hydroxyl group of the catalyst. The benzaldehyde is subject to the nucleophilic attack by the base sites on the boron nitride to form an imine intermediate. The imine intermediate reacts with deprotonated nitromethane, resulting in the formation of nitroalkene. Originally, this acid-base bifunctional mechanism was proposed for aminosilica catalysts,^[33,34] and the same mechanism can be adopted for the boron nitride catalyst having amino- and hydroxyl groups.^[30] Owing to the acid-base bifunctionality, the boron nitride catalyst exhibited higher activity than γ -Al₂O₃ though both had comparable basicity.

Table 4. Nitroaldol reaction of nitromethane and various substituted benzaldehyde using BN(1:5) catalyst^[a]

| Substrate | Hammett constant σ | Reaction rate /mmol g ⁻¹ h ⁻¹ |
|--|---------------------------|---|
| <i>p</i> -Methoxy benzaldehyde (1a) | -0.268 | 0.27 |
| <i>m</i> -Methoxy benzaldehyde (1b) | 0.115 | 0.20 |
| Benzaldehyde (1c) | 0 | 0.15 |
| <i>p</i> -Tolualdehyde (1d) | -0.17 | 0.20 |
| <i>p</i> -Chloro benzaldehyde (1e) | 0.227 | 0.22 |

[a] Reaction conditions: **1** (0.5 mmol), **2** (1.25 mmol), BN(1:5) (50 mg), *n*-decane (0.1 mmol), toluene (2 mL), 393 K.

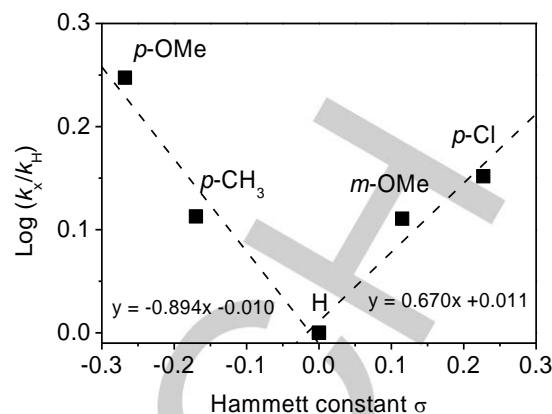
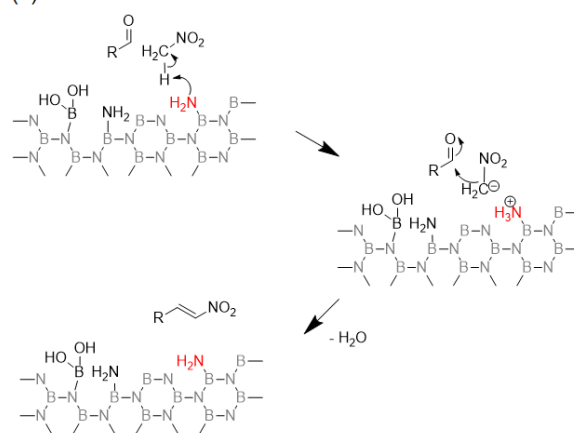
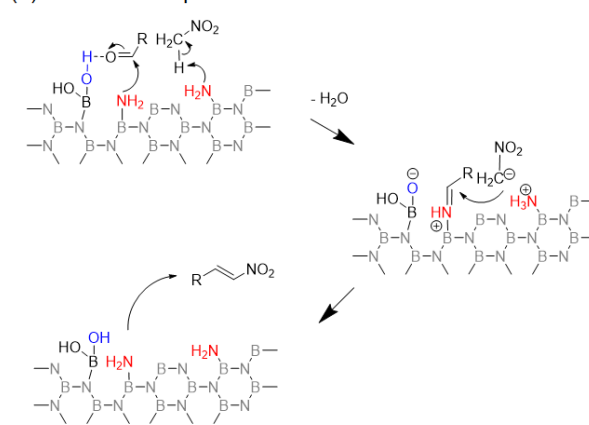


Figure 8. Results of the Hammett plot for the nitroaldol reaction

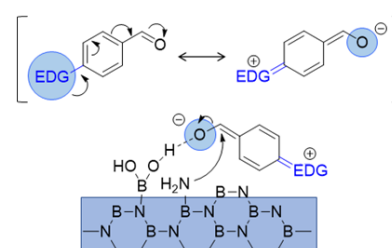
(a) Base mechanism



(b) Acid-base cooperative mechanism



(c) Resonance effect



Scheme 2 Proposed reaction mechanism of nitroaldol reaction. (a) base mechanism, (b) acid-base cooperative mechanism, and (c) resonance effect.

The correlation between the activities of the catalysts and their characteristics was investigated. Figure 9(a) shows the conversion of **1a** over various boron nitride catalysts. The conversion increased from BN(1:2) to BN(1:5) and then decreased. This trend is close to that for the pore volume of the catalyst, shown in Figure 3(d). A good correlation was obtained between conversion and pore volume (Figure 9(b)). Having a high porosity is important for increasing the catalytic activity. In addition, the correlation between the solid base amount and the catalytic activity was examined. It was found that the conversion of **1a** increased with increasing the amount of base sites. The correlation among the amount of base sites, the pore volume, and the catalytic activity indicates that all boron nitrides tested have similar active sites within the pores. While the BN(1:5) showed the stronger base sites than other BN materials, its strong basicity seems to be not closely related to the catalytic activity because BN(1:5) and BN(1:10) showed the same turnover number, 38 for BN(1:5) and 37 for BN(1:10). In addition, it is considered that a change in the oxygen content was not directly correlated to the catalytic activity because amino groups are attributable to the main active base sites.

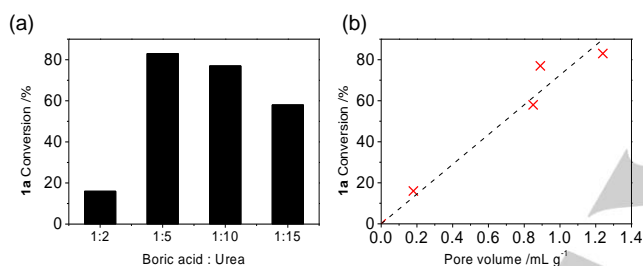


Figure 9. (a) conversion of **1a** over boron nitride and correlations between conversion of **1a** and (b) pore volume of boron nitride catalysts.

Conclusion

Boron nitride solid base catalysts were synthesized by a pyrolysis method using boric acid and urea at various molar ratios under NH₃ atmosphere. The samples prepared were highly porous turbostratic boron nitride and exhibited surface amino and hydroxyl groups with weak basicity. While BN(1:2), which had only micropores, gave a moderate activity for the nitroaldol reaction, BN(1:5), which possessed both micropores and mesopores, showed high activity with a high selectivity to nitroalkene, superior to those of conventional solid bases such as CaO and hydrotalcite. The porous structure of the boron nitride catalysts correlated strongly with their catalytic activity.

Experimental Section

Catalyst Preparation. The samples were synthesized by using boric acid (Kishida, 99.5%) and urea (Wako, 99.0%). 10 mmol of boric acid and 50 mmol of urea were dissolved in 100 mL of DI water, and the solution was evaporated to dryness. The obtained precursor powder (ca. 3 g) was transferred to an alumina boat and heated at 1273 K for 3 h in an NH₃ flow (100 cm³ (NTP) min⁻¹). Synthesis was also carried out using varying molar ratio of boric acid to urea, namely 1:2, 1:5, 1:10 and 1:15. The synthesized boron nitride is denoted as BN(1:n).

Characterization. The crystal structures of the boron nitride samples were determined by X-ray diffraction (XRD, RINT-2500HLR+, Rigaku) with Cu K α radiation ($\lambda = 0.15418$ nm) at a voltage of 40 kV and a current of 80 mA. Scans were obtained at a rate of 5° min⁻¹ with a step width of 0.05° for 2 θ values from 10° to 80°.

The surface morphologies of the samples were observed by scanning electron microscopy (SEM, JSM-7900F, JEOL). The elemental compositions of the samples were analyzed by energy dispersive X-ray spectroscopy (EDX, X-MaxN, Oxford). The surface functional groups of the samples were characterized by Fourier transform infrared spectroscopy (FTIR, FT/IR-6600, JASCO). The samples were pressed into pellets with KBr for the measurements. The solid base strength of the sample was determined by CDCl₃-adsorbed FTIR. For the adsorption measurement, a mercury cadmium telluride (MCT) detector with a resolution of 4 cm⁻¹ was used. Sample BN(1:5) was pressed into a disk with a radius of 1.0 cm without KBr and pretreated in the measurement cell at 473 K in vacuum for 1 h. The sample was cooled to 303 K, and a spectrum was recorded. CDCl₃ gas was introduced to the cell, and the sample was exposed to saturated CDCl₃ gas for 30 min. After CDCl₃ was pumped out for 30 min, a spectrum of the CDCl₃-adsorbed sample was measured. A difference spectrum was obtained by subtracting the spectrum of the dehydrated sample from the spectrum of the adsorbed sample.

The surface area was determined by the Brunauer-Emmett-Teller (BET) method using nitrogen adsorption (BELSORP-max-32-N-VP-CM and BELLSORP mini-II, Microtrac-BEL). The sample was pretreated by evacuation at 473 K for 2 h before the measurement. The pore size distribution of the sample was obtained by analyzing the adsorption branches of the isotherms through the Barrett, Joyner, and Halenda (BJH) method. A *t*-plot was used for micropore analysis. The B-K edge XAFS spectra were measured at beamline BL7A of the Photon Factory at the Institute of Materials Structure Science, High-Energy Accelerator Research Organization (KEK-IMSS-PF). The spectra were collected by the total electron yield method. Samples were mounted on carbon tape. All spectra were calibrated with reference to the B₂O₃ peak at 194.0 eV.

Nitroaldol reaction. The base catalytic activity of the sample was determined through the nitroaldol reaction. The nitroaldol reaction was conducted with the catalyst (50 mg) in 2 mL toluene solution containing *p*-methoxybenzaldehyde (60.5 μ L, 0.5 mmol), nitromethane (68.0 μ L, 1.25 mmol) and *n*-decane (19.5 μ L, 0.1 mmol) as an internal standard. The reaction was performed at 393 K, and aliquots were taken by syringe and analyzed by gas chromatography (GC-FID; GC-2014, column DB-1MS, Shimadzu).

Acknowledgements

This work was supported by a Grant-in-Aid for Science Research (B) (No. 18H01785) of JSPS, Japan. A part of this work was performed at the KEK-IMSS-PF (2017G529 and 2019G674).

Keywords: Nitrides • Nitroaldol reaction • Porous materials • Solid base catalyst • X-ray absorption spectroscopy

- [1] K. Tanabe, W.F. Hölderich, *Appl. Catal. A Gen.* **1999**, *181*, 399-434.
- [2] Y. Ono, H. Hattori, *Solid Base Catalysis*, Springer-Verlag, Berlin Heidelberg, **2011**.
- [3] a) J. T. Grant, C. A. Carrero, F. Goeltl, J. Venegas, P. Mueller, S. P. Burt, S. E. Specht, W. P. McDermott, A. Chierogato, I. Hermans, *Science* **2016**, *354*, 1570-1573; b) L. Shi, Y. Wang, B. Yan, W. Song, D. Shao, A.-H. Lu, *Chem. Commun.* **2018**, *54*, 10936-10946; c) L. Shi, D. Wang, W. Song, D. Shao, W.-P. Zhang, A.-H. Lu, *ChemCatChem* **2017**, *9*, 1788-1793; d) J.M. Venegas, J.T. Grant, W.P. McDermott, S.P. Burt, J. Micka, C.A. Carrero, I. Hermans, *ChemCatChem* **2017**, *9*, 2118-

- 2127; e) R. Huang, B. Zhang, J. Wang, K.-H. Wu, W. Shi, Y. Zhang, Y. Liu, A. Zheng, R. Schlögl, D.S. Su, *ChemCatChem* **2017**, *9*, 3293-3297.
- [4] Y. Wang, L. Zhao, L. Shi, J. Sheng, W. Zhang, X.-M. Cao, P. Hu, A.-H. Lu, *Catal. Sci. Technol.* **2018**, *8*, 2051-2055.
- [5] a) C. Huang, C. Chen, M. Zhang, L. Lin, X. Ye, S. Lin, M. Antonietti, X. Wang, *Nat. Commun.* **2015**, *6*, 7698; b) L. Chen, M. Zhou, Z. Luo, M. Wakeel, A.M. Asiri, X. Wang, *Appl. Catal. B Environ.* **2019**, *241*, 246-255.
- [6] a) R. Shankar, M. Sachs, L. Francàs, D. Lubert-Perquel, G. Kerherve, A. Regoutz, C. Petit, *J. Mater. Chem. A* **2019**, *7*, 23931-23940; b) Y. Cao, R. Zhang, T. Zhou, S. Jin, J. Huang, J. Ye, Z. Huang, F. Wang, Y. Zhou, *ACS Appl. Mater. Interfaces* **2020**, *12*, 9935-9943.
- [7] L. Dai, Y. Wei, X. Xu, P. Wu, M. Zhang, C. Wang, H. Li, Q. Zhang, H. Li, W. Zhu, *ChemCatChem* **2020**, *12*, 1734-1742.
- [8] a) X. Li, B. Lin, H. Li, Q. Yu, Y. Ge, X. Jin, X. Liu, Y. Zhou, J. Xiao, *Appl. Catal. B Environ.* **2018**, *239*, 254-259; c) J. Zhao, B. Lin, Y. Zhu, Y. Zhou, H. Liu, *Catal. Sci. Technol.* **2018**, *8*, 5900-5905; c) A. Takagaki, *Catal. Today* **2020**, *352*, 279-286.
- [9] W. Zhu, Z. Wu, G.S. Foo, X. Gao, M. Zhou, B. Liu, G.M. Veith, P. Wu, K.L. Browning, H.N. Lee, H. Li, S. Dai, H. Zhu, *Nature Commun.* **2017**, *8*, 15291.
- [10] P. Wu, Y. Wu, L. Chen, J. He, M. Hua, F. Zhu, X. Chu, J. Xiong, M. He, W. Zhu, H. Li, *Chem. Eng. J.* **2020**, *380*, 122526.
- [11] a) A. Nag, N. Raidongia, K.P.S.S. Hembram, R. Datta, U.V. Waghmare, C.N.R. Rao, *ACS Nano* **2010**, *4*, 1539-1544; b) S. Marchesini, C.M. McGilvery, J. Bailey, C. Petit, *ACS Nano* **2017**, *11*, 10003-10011.
- [12] X. Li, X. Wang, J. Zhang, N. Hanagata, X. Wang, Q. Weng, A. Ito, Y. Bando, D. Golberg, *Nat. Commun.* **2017**, *8*, 13936.
- [13] J. Li, K. Gao, *J. Mater. Chem.* **2003**, *13*, 628-630.
- [14] M.I. Baraton, T. Merle, P. Quintard, V. Lorenzelli, *Langmuir* **1993**, *9*, 1486-1491.
- [15] T. Sainsbury, A. Satti, P. May, Z. Wang, I. McGovern, Y.K. Gun'ko, J. Coleman, *J. Am. Chem. Soc.* **2012**, *134*, 18758-18771.
- [16] C. Huang, C. Chen, X. Ye, W. Ye, J. Hu, C. Xu, X. Qiu, *J. Mater. Chem. A* **2013**, *1*, 12192-12197.
- [17] Y. Chao, J. Zhang, H. Li, P. Wu, X. Li, H. Chang, J. He, H. Wu, H. Li, W. Zhu, *Chem. Eng. J.* **2020**, *387*, 124138.
- [18] I. Jiménez, A.F. Jankowski, L.J. Terminello, D.G.J. Sutherland, J.A. Carlisle, G.L. Doll, W.M. Tong, D.K. Shuh, F.J. Himpsel, *Phys. Rev. B* **1997**, *55*, 12025.
- [19] M.E. Fleet, S. Muthupari, *J. Non-Cryst. Solids* **1999**, *255*, 233-241.
- [20] A.M. Love, B. Thomas, S.E. Specht, M.P. Hanrahan, J.M. Venegas, S.P. Burt, J.T. Grant, M.C. Cendejas, W.P. McDermott, A.J. Rossini, I. Hermans, *J. Am. Chem. Soc.* **2019**, *141*, 182-190.
- [21] W. Zhu, X. Gao, Q. Li, H. Li, Y. Chao, M. Li, S.M. Mahurin, H. Li, H. Zhu, S. Dai, *Angew. Chem. Int. Ed.* **2016**, *55*, 10766-10770.
- [22] S.P. Huber, E. Gullikson, R.W.E. van de Kruijs, F. Bijkerk, D. Prendergast, *Phys. Rev. B* **2015**, *92*, 245310.
- [23] Q. Weng, D.G. Kvashnin, X. Wang, O. Cretu, Y. Yang, M. Zhou, C. Zhang, D.-M. Tang, R.B. Sorokin, Y. Bando, D. Golberg, *Adv. Mater.* **2017**, *29*, 1700695.
- [24] M. Kasrai, M.E. Fleet, S. Muthupari, D. Li, G.M. Bancroft, *Phys. Chem. Minerals* **1998**, *25*, 268-272.
- [25] D. Li, G.M. Bancroft, M.E. Fleet, P.C. Hess, Z.F. Yin, *Am. Mineral.* **1995**, *80*, 873-877.
- [26] E.P. Paukshtis, N.S. Kostsarenko, L.G. Karakchev, *React. Kinet. Catal. Lett.* **1979**, *12*, 315-319.
- [27] P. Barteau, M.-A. Kellens, B. Delmon, *J. Chem. Soc., Faraday Trans.* **1991**, *87*, 1425-1431.
- [28] S. Huber, H. Knözinger, *J. Mol. Catal. A Chem.* **1999**, *141*, 117-127.
- [29] K. Akutsu, H. Kabashima, T. Seki, H. Hattori, *Appl. Catal. A* **2003**, *247*, 65-74.
- [30] R. Devi, R. Borah, R.C. Deka, *Appl. Catal. A* **2012**, *433-434*, 122-127.
- [31] J.O. Schreck, *J. Chem. Edu.* **1971**, *48*, 103-107.
- [32] S. Torii, K. Jimura, S. Hayashi, R. Kikuchi, A. Takagaki, *J. Catal.* **2017**, *355*, 176-184.
- [33] J.D. Bass, A. Solovyov, A.J. Pascall, A. Katz, *J. Am. Chem. Soc.* **2006**, *128*, 3737-3747.
- [34] K. Motokura, M. Tada, Y. Iwasawa, *Angew. Chem. Int. Ed.* **2008**, *47*, 9230-9235.

